Pseudo-spin quantum computation in semiconductor nanostructures

New Journal of Physics
The open–access journal for physics

Pseudo-spin quantum computation in semiconductor nanostructures

V W Scarola, K Park and S Das Sarma
Condensed Matter Theory Center, Department of Physics,
University of Maryland, College Park, MD 20742, USA
E-mail: scarola@physics.umd.edu

New Journal of Physics **7** (2005) 177
Received 25 February 2005
Published 26 August 2005
Online at http://www.njp.org/
doi:10.1088/1367-2630/7/1/177

Abstract. We review the theoretical aspects of pseudo-spin quantum computation using vertically coupled quantum dots in the quantum Hall regime. We discuss the robustness and addressability of these collective, charge-based qubits. The low-energy Hilbert space of a coupled set of qubits yields an effective quantum Ising model tunable through external gates. An experimental prediction of an even–odd effect in the Coulomb-blockade spectra of the coupled quantum dot system allows for a probe of the parameter regime necessary for realization of these qubits.

Contents

PII: S1367-2630(05)95327-5

1. Introduction

Implementation of useful quantum algorithms requires large-scale quantum information processing. One perceived advantage of solid-state quantum computing proposals has been the possibility of scaling up the system to produce nearly homogeneous arrays of qubits with tunable interactions. Some rather promising proposals [1, 2] make use of real spin in semiconductor nanostructures as a natural two-level system with tunable couplings. A potential advantage of real spin quantum computation over charge-based proposals is the long decoherence times for spin states in solids, $\sim\mu$s or longer. One particular demerit of these proposals is the difficulty in addressing a single spin. Experimental techniques required to perform local manipulation of a single spin through applied magnetic fields push the limits of current technology [3]. Similarly, single-spin detection has proven difficult. Recent experiments [4]–[7] involving single-spin detection have shown some success. These measurements are an important step in quantum computing with real spins but remain far from the goal of measuring several individual spins at specific locations.

An interesting solid-state quantum computing implementation [8, 9] makes use of the coherent properties of bilayer quantum Hall states confined to nanostructures offering the possibility of charge-based quantum computing with long decoherence times. Charge-based proposals yield the advantage of addressability. Detection and manipulation of individual charges in quantum dots with single electron transistors is the standard practice [10, 11]. Single charges in the solid state, however, are particularly sensitive to electric field fluctuations, phonons, and other very strong and common noise sources in solids. As we will discuss below, the charge degree of freedom in quantum Hall states comprises many-body states which map onto a pseudo-spin and remain robust against external perturbations. The quantum Hall liquid is incompressible and, by definition, possesses a gap to excited states in the charge sector. Quantum Hall states confined to nanostructures [12]–[14] therefore offer a many-body charge-based qubit which should be less susceptible to certain types of environmental noise than similar systems using single charges. These systems are in direct analogy to the Cooper pair box system [15]–[17] (another solid state, charge-based qubit) as a mesoscopic, scaled-down version of a coherent, bulk condensate in the solid state.

In what follows, we review the microscopic theory and fundamental aspects of pseudo-spin quantum computing using bilayer quantum Hall systems confined to nanostructures [8, 9, 18]. In section 2, we discuss the coherent properties of bilayer quantum Hall systems. We draw an analogy between exciton condensation in these systems and low-temperature superconductivity. In section 3, we discuss the microscopic theory used to model vertically coupled quantum dots in the quantum Hall regime. We discuss the parameters necessary to define a two-level system. In section 4, we construct an effective, single pseudo-spin model for the qubit. We outline several theoretical results which compare noise issues of the many-body pseudo-spin qubits discussed here with similar single-charge qubits. In section 5, we review a derivation of a low-energy, pseudo-spin model describing Coulomb-coupled pseudo-spin qubits. The resulting quantum Ising model is sufficient for carrying out a universal set of quantum gates on a set of pseudo-spin qubits. In section 6 we present the conclusions of the paper.

2. Exciton condensation in bilayer quantum Hall systems

In this section we review the physics of exciton condensation in 'bulk' quantum Hall bilayers. We discuss the geometry, formalism and phenomena in the bulk that will be relevant for our discussion of pseudo-spin quantum computation using a scaled-down version of the bulk system: vertically coupled quantum dots in the quantum Hall regime. The bulk system consists of two parallel two-dimensional electron gases separated by a barrier of thickness ∼10–100Å, for example. A magnetic field oriented perpendicular to the plane quantizes the planar motion of electrons into Landau levels (LLs). Along the direction perpendicular to the two-dimensional plane, the electrons lie in the lowest subband of the confinement potential. The finite extent of the wavefunctions in the perpendicular direction allows for a small amount of single-particle tunnelling, t, between the two two-dimensional electron gases. (The tunnelling is equal to the symmetric–antisymmetric gap established by the double quantum well confining the electrons perpendicular to the plane.) At low tunnelling, the interlayer physics is dominated by the Coulomb interaction. Even without single-particle tunnelling, the two layers correlate through the Coulomb interaction. In fact the large Coulomb interaction, along with the large magnetic fields in these systems, polarizes the real electron spin in parameter regimes where the ground state is essentially ferromagnetic. In what follows we take the system to be fully real-spin polarized.

Transport experiments on quantum Hall bilayers display a variety of spectacular phenomena [19]. We discuss results associated with magnetic fields large enough to produce one flux quanta per electron, i.e. total filling $\nu_T = 1$. Interlayer tunnelling conductance measurements at this filling [20] reveal a dramatic increase in tunnelling conductance. The dramatic increase has been associated with a spontaneously interlayer coherent phase supported by an equal number of electrons and correlation holes residing in each of the two-dimensional layers [19]. The resulting exciton condensate has been the subject of intense theoretical and experimental study [19, 21].

The fundamental properties of this neutral superfluid have been well established [19]. We begin with a Hamiltonian describing electrons confined to bilayer systems:

$$H = \frac{1}{2m^*}\sum_j \left(\mathrm{i}\hbar\nabla_j - \frac{e}{c}\boldsymbol{A}_j\right)^2 + V_C + H_t, \tag{1}$$

where the interaction is given by

$$V_C = \frac{e^2}{2\epsilon}\sum_{(i,j);(\alpha,\beta)}{}' \frac{1}{\sqrt{|\boldsymbol{r}_i^\alpha - \boldsymbol{r}_j^\beta|^2 + d^2(1-\delta_{\alpha,\beta})}}. \tag{2}$$

Here m^* is the electron-effective mass, ϵ the dielectric constant of the host material and d the centre-to-centre interlayer separation. The indices $\alpha, \beta \in \{\uparrow, \downarrow\}$ denote layer index (up or down) while the prime on the sum indicates $i \neq j$ when $\alpha = \beta$. We work in the symmetric gauge at magnetic field B: $\boldsymbol{A} = \frac{B}{2}(y, -x)$. H_t, in equation (1), denotes the interlayer tunnelling Hamiltonian which we take to be small.

The single particle energy spectrum is split into LLs. The splitting is given by $\hbar\omega_c$, where $\omega_c = eB/m^*c$. At large fields the kinetic energy is quenched to the lowest LL. The basis states are given by

$$\phi_m = (2\pi 2^m m!)^{-1/2}\left(\frac{z}{l_B}\right)^m \exp\left(-|z|^2/4l_B^2\right), \tag{3}$$

where the planar coordinates, $z = x + \mathrm{i}y$, scale with the magnetic length $l_B = (\hbar c/eB)^{1/2}$. The quantum number m represents the angular momentum. It is the eigenvalue of the angular momentum operator: $\hat{L}_z = z\partial_z - z^*\partial_{z^*}$. When recast in the basis of the lowest LL the problem simplifies. Estimates [22] of the effects of LL mixing (along with finite thickness perpendicular to the plane) find, at most, a 15% correction to energy differences. In what follows, we ignore finite thickness and LL mixing.

At $\nu_T = 1$, the Hartree–Fock solution of equation (1) provides a surprisingly accurate solution over a large range of parameters, $d/l_B \lesssim 1.5$. The layer index enlarges the Hilbert space. A Hund's rule, applicable to layer index, picks out a single low-energy state, the ground state in the Hartree–Fock approximation, to minimize the Coulomb energy cost. The total ground state wavefunction, including the orbital and layer degrees of freedom, is generally given by $\Psi = \mathcal{A}[\prod_{\{\alpha\},\{m\}} \phi_m \chi_\alpha]$. Here $\mathcal{A}$ is the antisymmetrization operator and χ a spinor dependent on the set of all layer indices $\{\alpha\}$. The orbital part takes a simple form [23]:

$$\psi_{S_z} \sim \prod_{r,s}(z_r^{\uparrow} - z_s^{\downarrow}) \prod_{i<j}(z_i^{\uparrow} - z_j^{\uparrow}) \prod_{i'<j'}(z_{i'}^{\downarrow} - z_{j'}^{\downarrow}) \exp\left(-\sum_{i,\alpha} |z_i^{\alpha}|^2/4l_B^2\right). \tag{4}$$

This solution represents the exact orbital part of the ground state in the limit $B \to \infty$ and $d/l_B \to 0$. This limit ensures our lowest LL projection while effectively lowering the interlayer separation in units of l_B. From this form of the wavefunction, we see that each electron lies opposite to a correlation hole in the neighbouring layer. The electron and its opposing zero form a neutral electron–hole pair. These excitons condense to form an exciton condensate associated with a spontaneously broken symmetry, discussed below.

The spinors in the total wavefunction suggest a pseudo-spin interpretation of the layer index. We formally define the pseudo-spin to be

$$\hat{\boldsymbol{S}} = \tfrac{1}{2} \sum_m c_{m,\alpha}^{\dagger} \boldsymbol{\sigma}_{\alpha\beta} c_{m,\beta}, \tag{5}$$

where $c_{m,\alpha}^{\dagger}$ creates an electron in layer α with orbital angular momentum m, and $\boldsymbol{\sigma}$ are the usual Pauli matrices. With this definition, the eigenvalue of the pseudo-spin operator along the pseudo-spin z direction, $S_z = (N_\uparrow - N_\downarrow)/2$, denotes the relative number difference between layers. Along the pseudo-spin x direction, the pseudo-spin operator is equivalent to the interlayer tunnelling operator. $\hat{S}_x$ creates a bonding state between layers. The pseudo-spin operator along the pseudo-spin y direction, $\hat{S}_y$, is equivalent to an interlayer current operator.

Consider a bilayer system with an interlayer bias adjusted to ensure an equal number of electrons in each layer, on average. The many-body ground state will consist of a coherent superposition of orbital states ψ_{S_z} centred around $S_z = 0$. The electrons and zeros swap places in a coherent fashion, enhancing the interlayer tunnelling in the process. The coherent properties of the ground state can be seen explicitly in its second-quantized form:

$$\prod_m [1 + c_{m,\uparrow}^{\dagger} c_{m,\downarrow}] \prod_{m'} c_{m',\uparrow}^{\dagger} |0\rangle. \tag{6}$$

	superconductors	bilayer quantum Hall systems at ν=1
origin of gap	e–e pairing	e–h pairing
fluctuation	number of Cooper pairs	relative number difference between the two layers: $2S_z$
coherence (Josephson effect)	coherent superposition between systems of N and N+1 Cooper pairs	coherent superposition between systems of S_z and S_z+1
mesoscopic version	superconducting grains (Cooper pair box)	vertically coupled quantum dots under magnetic field (quantum Hall droplets)

Figure 1. Table summarizing the analogous properties of superconductors and exciton condensation in bilayer quantum Hall systems.

This ground state has a form similar to the well-known Bardeen–Cooper–Schrieffer (BCS) ground state of a superconductor:

$$\prod_k [u_k + v_k c^\dagger_{k,\uparrow} c^\dagger_{-k,\downarrow}]|0\rangle, \tag{7}$$

where k denotes a wave vector, the arrows indicate real spin (in equation (7)) and the coefficients u and v are fixed to ensure proper relative phases. By comparison we see that, with a redefined vacuum ($\prod_{m'} c^\dagger_{m',\uparrow}|0\rangle \to |0\rangle$), the excitons condense to form a neutral superfluid analogous to the condensation of Cooper pairs in a BCS superconductor. Equation (6) describes a coherent superposition of eigenstates of pseudo-spin centred around $S_z = 0$, while the BCS state captures a coherent superposition of number eigenstates.

Exciton condensation is associated with a spontaneous breaking of pseudo-spin symmetry. The electrons must have some (albeit arbitrarily small) interlayer, single-particle tunnelling to enable passage between layers. But even with an infinitesimally small amount of tunnelling, $t/(e^2/\epsilon l_B) \to 0$, the system, in the coherent ground state, exhibits a large tunnelling renormalized by the interaction:

$$\lim_{t\to 0} \langle \Psi | \hat{S}_x | \Psi \rangle \sim N/2, \tag{8}$$

where N is the total number of particles. An arbitrarily small amount of tunnelling spontaneously reorients the total pseudo-spin along the pseudo-spin x direction. The observation [20] of enhanced interlayer conductance, at $\nu_T = 1$, suggests the formation of an exciton condensate with an order parameter defined by equation (8).

By analogy with superconductivity, one may consider the mesoscopic version of the exciton condensate. The mesoscopic version of a BCS superconductor is a superconducting grain which exhibits some of the coherent properties of superconductors but in a smaller system. Vertically separated, lateral quantum dots in the quantum Hall regime offer the 'mesoscopic' version of the bulk exciton condensate discussed above. Figure 1 summarizes the analogous properties of

exciton condensates and superconductors. In what follows we discuss the possibility of encoding quantum information in the layer degree of freedom of a mesoscopic exciton condensate. In the next section, we discuss the properties of an individual qubit and the experimental prediction of an even–odd effect in the Coulomb-blockade spectra caused by spontaneous interlayer phase coherence inherent in our qubit.

3. Bilayer quantum Hall droplets

We now define the model and parameter regime necessary to establish a robust two-level system in a mesoscopic version of the exciton condensate discussed above. We review a proposal [18] designed to characterize the two-level system and quantitatively test the interlayer coherence present in the system. An even–odd effect in the Coulomb-blockade spectra of such a device yields an accurate test of interlayer coherence and, as we will see, provides important information related to the two-level systems encoded in the pseudo-spin degree of freedom.

Consider a bilayer quantum Hall system at $\nu_T = 1$ with vanishingly small interlayer tunnelling, as described in the previous section. The application of an external confinement fixes the total number of particles $N = N_\uparrow + N_\downarrow$. It is sufficient to consider parabolic confinement:

$$H_{\omega_0} = \tfrac{1}{2} m^* \omega_0^2 \sum_i |\boldsymbol{r}_i|^2, \tag{9}$$

where the confinement parameter, $\hbar\omega_0 = 3$–8 meV in GaAs samples, can be adjusted with external gates. In the presence of a parabolic confinement, the single particle eigenstates of the non-interacting Hamiltonian are the Fock–Darwin states [24, 25]. In the large magnetic field limit, $\omega_c \gg \omega_0$, the eigenstates reduce to equation (3) but with the replacement: $l_B \to a$, where we define the modified magnetic length, $a \equiv l_B(1 + 4\omega_0^2/\omega_c^2)^{-1/4}$. These states provide a basis for our calculations.

With a small number of particles $N \sim 1$–100, the system forms a maximum density liquid with an equal number of particles and flux quanta piercing the system. This few-body state, often called the maximum density droplet (MDD), is separated from the excited states by a gap. It is the mesoscopic realization of the bulk $\nu_T = 1$ quantum Hall state, equation (4). In the special case of an odd number of particles, the two degenerate low-energy states have total pseudo-spin $S_z = \pm 1/2$. The + (−) indicates one excess charge in the top (bottom) layer. These two states, denoted $|\pm 1/2\rangle$, define a two-level system arising from a competition between the Coulomb interaction and confinement. An even number of particles distributed between the two layers yields one state with $S_z = 0$.

We study the low-energy physics of a bilayer quantum Hall droplet (BQHD) with an odd number of particles using exact diagonalization. In second quantization, the lowest LL Hamiltonian describing the system, including confinement and finite tunnelling now reads:

$$H_{LLL} = \gamma \sum_{m,\alpha} m c^\dagger_{m,\alpha} c_{m,\alpha} + \sum_{\{m\},(\alpha,\beta)} V^{\alpha,\beta}_{\{m\}} c^\dagger_{m_1,\alpha} c^\dagger_{m_2,\beta} c_{m_3,\beta} c_{m_4,\alpha} - t\hat{S}_x, \tag{10}$$

where the confinement redefines the basis length scale and adds the first term with coefficient $\gamma \equiv \hbar(\sqrt{\omega_c^2 + 4\omega_0^2} - \omega_c)/2$. Explicit expressions for the Coulomb matrix elements, $V^{\alpha,\beta}_{\{m\}}$, can be found in the literature [26, 27]. We diagonalize the system in the limit $t = 0$ and consider

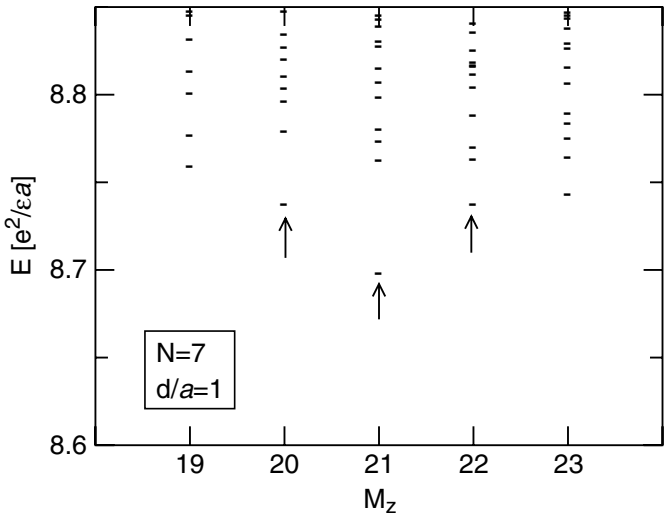

Figure 2. Energy spectrum as a function of total angular momentum for a bilayer quantum Hall droplet with four (three) electrons in the top (bottom) layer, $S_z = +1/2$. The energies are obtained from exact diagonalization of equation (10) with tunnelling, $t = 0$, interlayer separation, $d = a$, and $\gamma = 0.1187e^2/\epsilon a$. We define the parameter $\gamma \equiv \hbar(\sqrt{\omega_c^2 + 4\omega_0^2} - \omega_c)/2$ and the modified magnetic length $a \equiv l_B(1 + 4\omega_0^2/\omega_c^2)^{-1/4}$ in terms of the confinement parameter, ω_0, the cyclotron frequency, ω_c, and the magnetic length $l_B = (\hbar c/eB)^{1/2}$. The arrows indicate the three lowest energy states. The central arrow indicates the $|+1/2\rangle$ state of our qubit (from [18]).

finite tunnelling effects subsequently. In this limit, the total z component of pseudo-spin, S_z, the total angular momentum, M_z, and the total particle number are all good quantum numbers. The first two terms in equation (10) compete. It is necessary to tune the magnetic field and confinement to the proper values ensuring that the MDD is the ground state of the system. The angular momentum of the MDD (the orbital state defined by equation (4)) is $M_z = N(N-1)/2$. With $N = 7$, for example, we find that a range of confinements centred around $\gamma = 0.1187e^2/\epsilon a$ yields the MDD ground state. Figure 2 plots the low-energy Hilbert space of equation (10) for $N = 7$ with $t = 0$ in the $S_z = +1/2$ sector as a function of total angular momentum. This implies four (three) electrons in the top (bottom) layer. The interlayer separation is chosen to be $d = a$. The arrows indicate the three lowest energy states. The central arrow shows the $|+1/2\rangle$ ground state. The left- and rightmost arrows indicate the edge excitations. It was found in [18] that the gap-to-edge excitations remains finite for $d/a \lesssim 2.0$. The many-body ground state found here is one of the two degenerate states which form a two-level system, separated from excited states (with the same S_z) by $\sim 0.07e^2/\epsilon a$ at $d = a$.

For an odd number of particles, BQHD states with $S_z = \pm 1/2$ have the lowest charging energy cost. They are separated from states with higher $|S_z|$ by the relative charging energy cost: $\alpha \hat{S}_z^2/N$, where we find $\alpha/(e^2/\epsilon a) \simeq -0.18 + 0.35d/a$ [18] for $d/a \gtrsim 0.5$ through an empirical fit to our numerical, exact diagonalization over several values of N. We find that for $d \approx a$, the two-level system defined by $|\pm 1/2\rangle$ remains separated from excited states by an energy $\sim 0.05e^2/\epsilon a$.

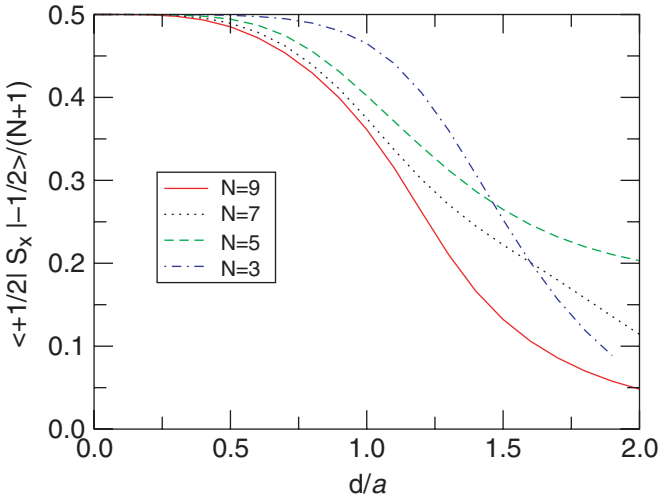

Figure 3. The interlayer coherence measure, as defined in equation (11), plotted as a function of inter-layer distance for several particle numbers with zero tunnelling.

We now discuss the coherence properties of a BQHD in the MDD state. As for the bulk system, the BQHD will develop a renormalized tunnelling gap: $\Delta_x = t\langle +1/2|\hat{S}_x| - 1/2\rangle$, in the limit $t/(e^2/\epsilon a) \to 0$. The Coulomb interaction enhances the single-particle tunnelling by a factor of order N. The definition of spontaneous interlayer phase coherence in the BQHD is then

$$\lim_{t\to 0} \frac{\Delta_x}{t} = \lim_{t\to 0} \langle +1/2|\hat{S}_x| - 1/2\rangle \neq 0. \tag{11}$$

In figure 3 we plot Δ_x/t as a function of interlayer separation for several odd particle numbers in the MDD state. We find Δ_x to be sizable for $d/a \lesssim 1.0$. The quantity Δ_x provides a mesoscopic measure of spontaneous interlayer phase coherence with direct experimental relevance.

The coherence order parameter, Δ_x, may be related to the Coulomb-blockade peak spacing measured in experiments on BQHDs. Coulomb-blockade peaks in the tunnelling conductance of quantum dots arise when the gate voltage, V_g, is tuned so that the total energy of the N-electron system coincides with the energy of the $(N+1)$-electron system. The total energy of the bilayer quantum dot system includes the total charging energy cost:

$$H_C = \frac{e^2}{2C_\Sigma}\left(N - \frac{CV_g}{e}\right)^2, \tag{12}$$

where C_Σ is the total capacitance of the double dot system and C is the lead capacitance to one of the two dots. The enhanced tunnelling gap leads to a splitting between hybridized states formed from the states $|\pm 1/2\rangle$ in systems with N odd, thereby modifying the total energy of the system (see figure 4). For an even number of particles no such splitting exists. There is only one state which minimizes the charging energy cost giving $\langle 0|\hat{S}_x|0\rangle = 0$. Therefore, the Coulomb-blockade peak spacing will alternate with an even or odd number of particles. Figure 4 illustrates the even–odd effect in BQHDs where the top panel, figure 4(a), shows the situation

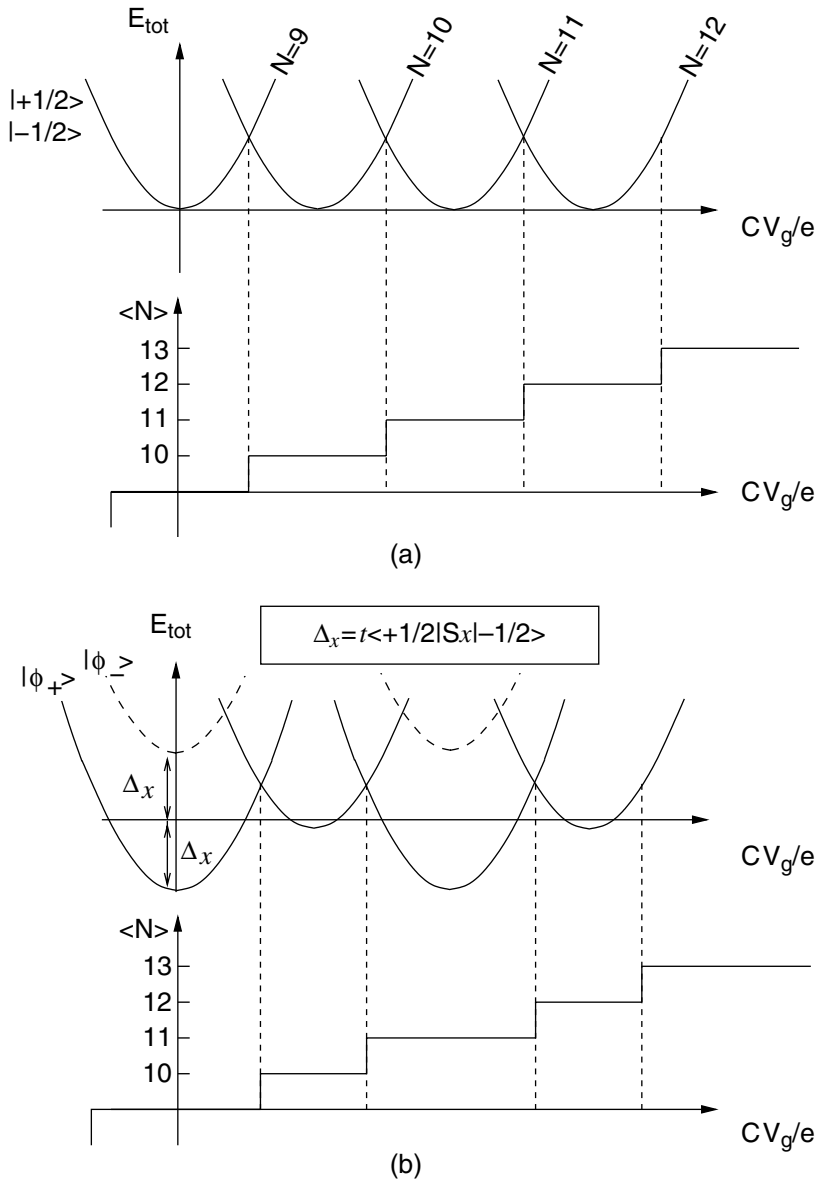

Figure 4. Schematic representation depicting the even–odd effect in BQHDs. The total energy is plotted as a function of CV_g/e, where V_g is the gate voltage and C the lead-dot capacitance. The total energy includes the charging energy. The average number of electrons distributed between the two dots is denoted $\langle N \rangle$. The top panel, (a), depicts the situation where there is no interlayer coherence. The states $|\pm 1/2\rangle$ are degenerate here. The bottom panel, (b), depicts the even–odd effect due to a coherence gap, Δ_x. The degenerate set of states here splits into symmetric and antisymmetric combinations $|\phi_+\rangle$ and $|\phi_-\rangle$.

with no interlayer coherence: $d/a \gg 1$. The bottom panel, figure 4(b), illustrates the even–odd effect arising from finite Δ_x. Observation of an even–odd effect in the Coulomb-blockade peak spacing would provide evidence for conditions sufficient to establish a two-level system in a BQHD.

4. Pseudo-spin qubits

The many-body two-level system defined by the states $|S_z = \pm 1/2\rangle$ in a BQHD offers a charge-based qubit with tunable effective magnetic fields. In this section we discuss two important aspects of BQHD qubits: the tunability and robustness of the qubit. The qubit proposal outlined here has several advantages and disadvantages in meeting the DiVincenzo criteria [28], as opposed to other solid-state quantum computing proposals. The disadvantages include susceptibility to leakage (as compared to real spin [1] which is inherently a two-level system) and charge noise. The advantages include ease of addressability (detection and manipulation of a single-electron charge, as opposed to a single-electron spin), tunability through externally applied electric fields and a certain rigidity against external perturbations (as compared to single-electron, charge-based qubits).

In the reduced Hilbert space $|\pm 1/2\rangle$ (as defined for a BQHD with an odd number of particles in the MDD state), two parameters may rotate the pseudo-spin. As noted previously, finite interlayer tunnelling effectively rotates the pseudo-spin along the pseudo-spin x direction. The parameter t can be tuned with external gates or by application of a real, in-plane magnetic field. Both fields alter the spread of the electron density along the direction perpendicular to the two-dimensional plane thereby tuning the interlayer overlap. These fields provide an effective magnetic field along the pseudo-spin x direction which is always negative.

An external bias, Δ_z, applied perpendicular to the two-dimensional plane of a BQHD energetically favours one pseudo-spin state over another. Δ_z acts as an effective magnetic field along the pseudo-spin z direction. We may therefore rotate the pseudo-spin direction through any point on the Bloch sphere by pulsing Δ_z and Δ_x. In the reduced Hilbert space, $|\pm 1/2\rangle$, we have a reduced Hamiltonian [8, 18]: $H_R = -\Delta_x \sigma_x + \Delta_z \sigma_z$. The collective state associated with an excess charge in either the top or bottom layer of a coherent BQHD in the MDD state therefore provides a fully tunable qubit.

Several potential error sources relevant for a BQHD qubit have been quantitatively addressed in the literature [8, 9]. Three types of error sources were studied in [8, 9]: (i) spatially local decoherence (ii) spatially global decoherence and (iii) leakage (as opposed to decoherence) due to density perturbations. The first type was studied in [8]. It was shown that phase flip errors arising from an inhomogeneous, externally applied potential are strongly suppressed by increasing the total number of particles defining the BQHD qubit. The results show that phase-flip errors are suppressed by more than an order of magnitude by increasing N from 1 to 10.

The second type of error was studied in [9]. The analysis of phase-flip errors arising from fluctuations in spatially homogeneous, external voltages in the leads (fluctuations in Δ_z) finds that, at low temperatures, the decoherence rate (the ratio of the dephasing rate to the elementary logic operation rate) can be made small enough to allow for fault-tolerant quantum computation. More precisely, we find the ratio to be $4[C/(2C + C_\Sigma)]^2 R_v/R_K$, where $R_v \sim 50\,\Omega$ is the typical impedance of the voltage circuit and $R_K = h/e^2$. The above analysis applies to voltage noise in leads attached to any charge-based qubit, pseudo-spin or otherwise, modelled in the spin-boson formalism. The above formula captures an implicit fact: isolating the system from the environment, $C \ll C_\Sigma$, can reduce the decoherence rate.

In addition to dephasing from voltage fluctuations, there is also the possibility of leakage due to density perturbations such as phonons. In [9] it was shown that increasing the particle number suppresses the form factor associated with phonons coupling the states $|\pm 1/2\rangle$ to unwanted edge

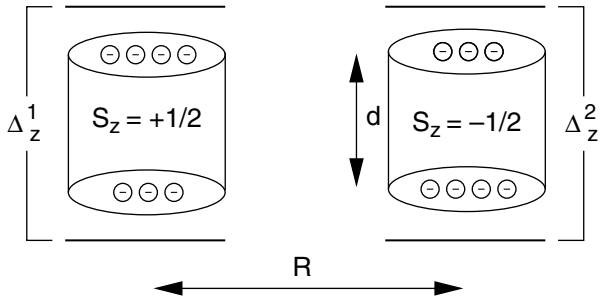

Figure 5. Schematic representation illustrating the low-energy state of Coulomb-coupled, neighbouring BQHDs separated by a centre-to-centre distance R. The configuration depicted here represents the pseudo-spin product state $|+1/2, -1/2\rangle$. The quantities Δ_z^i depict the applied bias on the ith set of quantum dots.

modes, $|e\rangle$. The form factor:

$$\left| \langle e | \sum_{j=1}^{N} \exp(\mathrm{i}\boldsymbol{k} \cdot \boldsymbol{r}_j) | \pm 1/2 \rangle \right|^2, \tag{13}$$

was suppressed by more than an order of magnitude in increasing N from 1 to 9. Here $\boldsymbol{k}$ is the wave vector of a density perturbation in the plane caused, for example, by a phonon of wave vector $\boldsymbol{k}$. We emphasize that the diminished form factor suppresses leakage due to any density perturbation, including both acoustic and optical phonons. The results of [8, 9] suggest that the rigidity inherent in collective and incompressible BQHD states suppress decoherence and leakage mechanisms otherwise present in single-electron, charge-based qubits in quantum dots.

5. Coulomb coupling

We now discuss the possibility of constructing a universal set of quantum gates by coupling BQHD qubits. There are several types of inter-BQHD couplings possible. Three examples are exchange, capacitive and Coulomb coupling. In what follows we discuss Coulomb-coupled BQHDs.

Consider two neighbouring BQHDs, as shown schematically in figure 5. The centres of the BQHDs are placed a distance R apart. The Coulomb interaction between neighbouring droplets will favour an anti-alignment of charge as depicted in figure 5. The charge distributes among two parallel disks with an excess of charge in the top (bottom) layer in the state $|+1/2\rangle$ ($|-1/2\rangle$). The disk extends to roughly the largest orbital state, $2\sqrt{N}a$. Figure 6 plots the density of two neighbouring BQHDs placed with a centre-to-centre distance of $R = 10a$. We obtain the densities from the exact diagonalization of equation (10) for a single BQHD with $t = 0, d = a$ and $N = 7$.

We consider the low-energy Hilbert space of two, well-separated BQHDs. The large inter-BQHD separation ensures little overlap between electronic states in neighbouring BQHDs. We also require that R is large enough so that a neighbouring BQHD does not induce unwanted intra-BQHD excitations. In this limit, the Hilbert space of two neighbouring BQHDs comprises a set

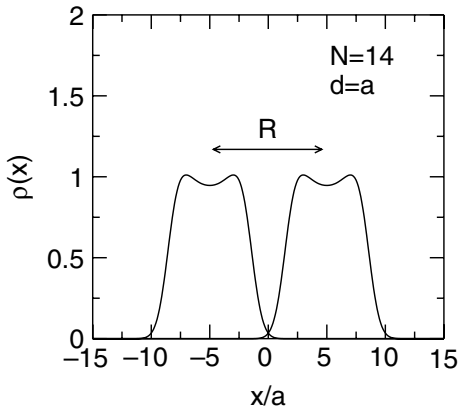

Figure 6. Normalized density profile versus lateral separation along the x-axis for a pair of BQHDs with a lateral separation $R = 10a$ in the maximum density droplet state, where a is a modified magnetic length defined in the text. The vertical inter-dot spacing is $d = a$. There are a total of 14 electrons distributed among all four droplets.

of four product states $\{|\pm 1/2, \pm 1/2\rangle, |\pm 1/2, \mp 1/2\rangle\}$. In this basis, the resulting inter-BQHD Coulomb interaction maps onto a pseudo-spin Ising interaction:

$$H_I = \frac{J}{2}\sigma_z^1\sigma_z^2, \tag{14}$$

where we define the effective exchange splitting to be

$$\begin{aligned} J = {} & \langle +1/2, +1/2|V(R, d; \boldsymbol{r}_i^{\alpha}, \boldsymbol{r}_j'^{\beta})|+1/2, +1/2\rangle, \\ & - \langle +1/2, -1/2 \mid V(R, d; \boldsymbol{r}_i^{\alpha}, \boldsymbol{r}_j'^{\beta}) \mid +1/2, -1/2\rangle, \end{aligned} \tag{15}$$

where

$$V(R, d; \boldsymbol{r}_i^{\alpha}, \boldsymbol{r}_j'^{\beta}) = \sum_{i,j} \frac{e^2}{\epsilon' a} \frac{1}{\sqrt{(x_i^{\alpha} - x_j'^{\beta} + R/a)^2 + (y_i^{\alpha} - y_j'^{\beta})^2 + (d/a)^2(1 - \delta_{\alpha,\beta})}}. \tag{16}$$

Here $\boldsymbol{r}$ ($\boldsymbol{r}'$) indicates the radial vector in the x–y plane in the left (right) BQHD and ϵ' is the inter-BQHD dielectric constant. At large distances, $R > 25a$, it was shown [9] that the 'exchange' coefficient exhibits dipolar behaviour, $J \propto R^{-3}$. However, at these large distances, we find J to be negligibly small in GaAs devices, leaving only nearest-neighbour interactions which can be tuned with ϵ' or R/a. Nonetheless, the long-range part of a dipolar coupling (albeit small) can give rise to errors in quantum gates constructed entirely from nearest-neighbour interactions. In [29] it was shown that errors due to dipolar coupling can be treated with quantum error correction gating schemes.

We generalize the double BQHD system to an arbitrary number of BQHDs. Each BQHD can be thought of as a lattice site i containing a pseudo-spin interacting with its neighbour through an Ising interaction:

$$H_I = \sum_i [-\Delta_x^i \sigma_x^i + \Delta_z^i \sigma_z^i] + \tfrac{1}{2} \sum_{i,j} J_{ij} \sigma_z^i \sigma_z^j. \tag{17}$$

The above model, with tunable coefficients, offers a universal set of quantum gates [30]. The effective magnetic fields are tunable through external electric fields. J is not so easily tuned. But an intermediate, idle BQHD with an odd or even number of electrons can turn the interaction between next-nearest neighbours on or off. Another possibility borrows techniques from nuclear magnetic resonance theory. It is well known that similar models with fixed inter-spin interactions allow quantum computation with refocusing pulses [31, 32].

6. Conclusion

We have reviewed the theoretical aspects of pseudo-spin quantum computation using confined, bilayer quantum Hall states. We argue that BQHDs offer the quantum Hall analogue of Cooper pair boxes. The even–odd effect in Coulomb-blockade spectra provides a criteria sufficient in defining a two-level system in the low-energy Hilbert space of a BQHD. The many-body, two-level system encoded in the layer degree of freedom provides advantages over single-charge-based qubits when considering external perturbations due to the environment. Coulomb coupling offers the possibility of a universal set of quantum gates through a pseudo-spin, quantum Ising model.

Acknowledgments

We would like to thank J K Jain for valuable discussions. We acknowledge support from ARDA and NSA-LPS.

References

[1] Loss D and DiVincenzo D P 1998 *Phys. Rev.* A **57** 120
[2] Kane B E 1998 *Nature* **393** 133
[3] Hu X, de Sousa R and Das Sarma S 2001 *Phys. Rev. Lett.* **86** 918
[4] Elzerman J M, Hanson R, van Beveren L H W, Wilfkamp B, Vandersypen L M K and Kouwenhoven L P 2004 *Nature* **430** 431
[5] Rugar D, Budakian R, Mamin H J and Chui B W 2004 *Nature* **430** 329
[6] Kroutvar M, Ducommun V, Heiss D, Bichler M, Schuh D, Abstreiter G and Finley J J 2004 *Nature* **432** 81
[7] Zumbuhl D M, Marcus C M, Hanson M P and Gossard A C 2004 *Phys. Rev. Lett.* **93** 256801
[8] Yang S R, Schliemann J and MacDonald A H 2002 *Phys. Rev.* B **66** 153302
[9] Scarola V W, Park K and Das Sarma S 2003 *Phys. Rev. Lett.* **91** 167903
[10] Ota T, Ono K, Stopa M, Hatano T, Tarucha S, Song H Z, Nakata Y, Miyazawa T, Ohshima T and Yokoyama N 2004 *Phys. Rev. Lett.* **93** 66801
[11] van der Wiel W G, De Franceschi S, Elzerman J M, Fujisawa T, Tarucha S and Kouwenhoven L P 2004 *Rev. Mod. Phys.* **75** 1
[12] Austing D G, Honda T, Muraki K, Tokura Y and Tarucha S 1998 *Physica* B **249–251B** 206
[13] Oosterkamp T H, Janssen J W, Kouwenhoven L P, Austing D G, Honda T and Tarucha S 1999 *Phys. Rev. Lett.* **82** 2931
[14] Rontani M, Amaha S, Muraki K, Manghi F, Molinari E, Tarucha S and Austing D G 2004 *Phys. Rev.* B **69** 85327
[15] Nakamura Y, Chen C D and Tasi J S 1997 *Phys. Rev. Lett.* **79** 2328
[16] Nakamura Y, Pashkin Yu A and Tsai J S 1999 *Nature* **398** 786

[17] Nakamura Y, Pashkin Yu A, Yamamoto T and Tsai J S 2002 *Phys. Rev. Lett.* **88** 047901
[18] Park K, Scarola V W and Das Sarma S 2003 *Phys. Rev. Lett.* **91** 026804
[19] Das Sarma S and Pinczuk A (ed) 1997 *Perspectives in Quantum Hall Effects* (New York: Wiley)
[20] Spielman I B, Eisenstein J P, Pfeiffer L N and West K W 2000 *Phys. Rev. Lett.* **84** 5808
[21] Eisenstein J P and MacDonald A H 2004 *Nature* **432** 691
[22] Price R and Das Sarma S 1996 *Phys. Rev.* B **54** 8033
[23] Halperin B I 1983 *Helv. Phys. Acta* **56** 75
[24] Fock V 1928 *Z. Phys.* **47** 446
[25] Darwin C G 1930 *Proc. Camb. Phil. Soc.* **27** 86
[26] Hawrylak P 1993 *Solid State Commun.* **88** 475
[27] Hawrylak P and Wojs A 1998 *Quantum Dots* (Berlin: Springer)
[28] DiVincenzo D 2000 *Fortschr. Phys.* **48** 771
[29] de Sousa R, Delgado J D and Das Sarma S 2004 *Phys. Rev.* A **70** 052304
[30] Barenco A, Bennett C H, Cleve R, DiVincenzo D P, Margolus N, Shor P, Sleator T, Smolin J A and Weinfurter H 1995 *Phys. Rev.* A **52** 3457
[31] Vandersypen L M K and Chuang I L 2004 *Rev. Mod. Phys.* **76** 1037
[32] Liu Yu-xi, Wei L F and Nori F 2004 *Preprint* quant-ph/0402179